Proceeding of the IEEE
International Conference on Robotics and Biomimetics
Dali, China, December 2019

Design and Yaw Control of a Two-Motor-Actuated Biomimetic Robotic Fish

Sheng Du[1,2], Zhengxing Wu[1,2], and Junzhi Yu[1,3]
[1]*State Key Lab Management and Control for Complex Systems, Institute of Automation, CAS, Beijing 100190, China*
[2]*University of Chinese Academy of Sciences, Beijing 100049, China*
[3]*Dept. Mech. Eng. Sci., BIC-ESAT, College of Engineering, Peking University, Beijing 100871, China*
{*dusheng2017, zhengxing.wu, junzhi.yu*}*@ia.ac.cn*

***Abstract*— This paper addresses the design and control of a novel tuna-inspired robotic fish able to realize both fast swimming and high maneuverability. A two-stage transmission mechanism is proposed, aiming at reducing the volume and mass of caudal peduncle. Benefited by it, both volumes and mass of moving parts can be reduced to allow higher swing frequency. At the same time, two joints driven by two motors ensure the flexibility of steering. The robotic fish achieves a maximum speed up to 1.65 body lengths per second (BL/s) and a minimum turning radius less than 0.35 body lengths (BL), based on the open-loop control designed by Central Pattern Generator (CPG) method. Furthermore, a yaw control is proposed to maintain course angle at high swimming speed, and simulation in Automatic Dynamic Analysis of Mechanical Systems (ADAMS) software reveals the effectiveness. The results show that the proposed yaw control method can regulate the fluctuation of anterior body to desired range but without compensation of sideways drift.**

***Index Terms*— Biomimetic robotic fish, fish swimming, yaw control, high maneuverability.**

I. Introduction

The underwater world is still mysterious to human beings. Though the traditional propeller driven Autonomous Underwater Vehicles (AUV) exist for many years, there are still many unsolved problems such as big noise and low energy utilization rate. Besides, the propeller is a threat to aquatic animals. For the undercurrent caused by rotating propeller makes aquatic animals hard to escape. Compared to the propeller driven AUV, biomimetic underwater robots are friendly to the surrounding environment. They achieve silenced and flexible locomotion as well [1]. However, the biomimetic underwater robots have their own problems, such as poor endurance and movement performance [2]. For example, fish has evolved a streamline body with mucus secretion to reduce water resistance, and strong muscular to interact with surrounding water. These features endow fish with remarkable abilities of high energy efficiency, high mobility, and precise yaw control. In nature, normal swimming speed of the fish is about 2.5–4 body length per second (BL/s) [3], and turn radius can be within 0.2 body length (BL). By contrast, biomimetic robotic fish is incapable of achieving the targets simultaneously.

Although there are many researches on ionic polymer-metal composite (IPMC) actuator, often called artificial muscle and other available actuators such as magnetic actuator and hydraulic/pneumatic drive [2], their performance are much poorer than the real muscle. In fact, these new drive modes are in the initial stage, and the performance are even defeated by the most common electric motor driven method.

In general, there are two ways to utilize the motor. One is the active wire/cable-driven method [4], and the other is the joint-driven method. The advantage of the former method is that the constructed robotic fish can swim more likely as a real fish, and it is easy to control. This method makes it possible to use one motor to drive multiple joints through flexible wires by meticulous design. Here the wires are used to imitate the muscle. But on the other hand, the flexibility of the wires makes it difficult to realize precise control. Besides, when a wire/cable-driven robotic fish is constructed, the mutual relation between joint angles are confirmed. Thus, the wire/cable-driven robotic fish can not achieve complex actions which need multiple-joint cooperation.

In the joint-driven method, joint angles are exactly determined by the motors. Compare to the wire/cable-driven method using flexible transmission mechanism, it uses a rigid one to ensure the precise control. Take the iSplash series [5], [6] for instance, they are designed to actuate two or more joints by one motor, but all parts of the transmission mechanism are rigid, implying that the joint angles are completely determined by the motor. As a comparison, the actual joint angles of a wire/cable-driven robotic fish are determined by both surrounding water force and the motor. Benefitting from the well-designed structure, the iSplash-II reaches a maximum speed of 11.6 BL/s at 20 Hz [6]. However, due to the feature that all joint angles are determined by a single motor, the iSplash-II lacks the ability of turning.

The common application of joint-driven method is that one motor drives one joint [7]–[11]. In this way, the robotic fish can realize complex actions by mutual cooperation between

*This work was supported by National Natural Science Foundation of China (Grant Nos. 61603388, 61725305, 61633017), Key Project of Frontier Science Research of Chinese Academy of Sciences (Grant No. QYZDJ-SSW-JSC004), and Pre-Research Fund of Equipments of China (Grant No. 61403120108).

978-1-7281-6321-5/19//$31.00 ©2019 IEEE

TABLE I

SWIMMING PERFORMANCE COMPARISON AMONG TYPICAL ROBOTIC FISHES

Platform	Number of active joints	Unified speed (BL/s)	Turning radius (BL)
iSplash-II [6]	1	11.6	Unavailable
BoxyBot [12]	1	1.4	0.5
PRC swimmer [13]	2	1.69	0.92
SPC-III [14]	2	1.1	1.4
Essex G9 [15]	3	1.02	0.3
CAS robotic fish [16]	4	1.04	0.23

motors. Usually, more motors make the robot more flexible, but affect the straight swimming speed, due to the increased weight of moving parts. It is a question worth considering that how many motors are needed to drive a robotic fish and how these motors cooperate with each others.

Previous studies confirm this view. As the Table I shows, based on the joint-driven method, more motors make the robotic fish more flexible, achieving a smaller turn radius, but largely decrease the maximum forward swimming speed. Conversely, less motors yield a higher speed but worse performance on maneuverability.

In this paper, we develop a novel two-motor-actuated robotic fish capable of both fast forward swimming and high maneuverability. Furthermore, a yaw control is proposed to deal with negative factors caused by the undulate motion, with the purpose of keeping stable course angle at high speed. The simulation result indicates the effectiveness of the proposed method.

The remainder of this paper is organized as follows. Section II introduces the mechanical design of the robotic fish. The open-loop control method and experiment results are presented in Section III. In Section IV, the yaw control is proposed, with simulation and analysis provided. Section V summarizes the conclusions.

II. MECHANICAL DESIGN OF THE ROBOTIC FISH

As discussed previously, more motors decrease the swimming speed but increase the precision and efficiency of turning motion. To retain both, a transmission mechanism adopting a two-motor-actuated method is designed. As a result, the problem that added motors increase the weight of moving parts in traditional series structure is solved.

Inspired by tuna, as Fig. 1 shows, our robotic fish mainly consists of three parts, a rigid anterior body, a light posterior body, and a lunate caudal fin. The anterior body, made of Acrylonitrile Butadiene Styrene (ABS), contains most of mechatronic parts such as two DC motors for waist and caudal joints, communicate units, a pair of pectoral fins, control boards, batteries, etc. The external profile of the anterior body imitates a real tuna, which is well-streamlined to reduce water resistance.

TABLE II

TECHNICAL SPECIFICATION OF THE ROBOTIC FISH

Parameters	Description
Dimensions	460 mm (L) × 100 mm (W) × 130 mm (H)
Weight	1.8 kg
Number of the active joints	2
Maximum swimming speed	1.65 BL/s
Minimum turning radius	0.35 BL
Power source	22.2 V and 7.4 V Li-ion batteries
Control mode	Radio control (433 MHz)

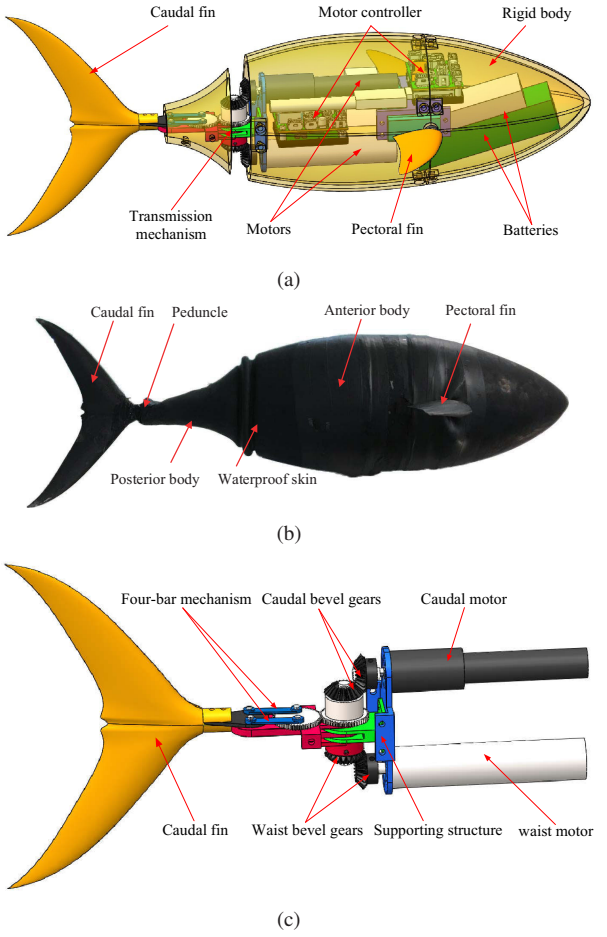

Fig. 1. Illustrations of the robotic fish. (a) Conceptual design. (b) Robotic prototype. (c) Transmission mechanism.

The posterior body, made of ABS, contains a light transmission mechanism used to drive the caudal joint. Benefit from the parallel layout of motors, the posterior shell is shaped dramatically shrunk from the anterior body to caudal fin, as the real tuna. As a result, the hydrodynamic drag caused by posterior shell moving in the water and the mass of the undulation parts are reduced to minimize.

The tuna is a typical thunniform swimmer, whose caudal fin provides the main propulsive force. The caudal fin made of polypropylene (PP) is designed with a large aspect ratio

as the same as a real tuna's fin, aiming at a higher swimming speed. As depicted in Fig. 1(c), the transmission mechanism is designed as two stage transmission. Firstly, the caudal motor actuates the caudal bevel gears, then the power is transmitted to caudal fin by a four-bar mechanism. The passive bevel gears are coaxial, which ensures that there is a linear relationship between two rotations. In this design, two joints are still driven by two motors, but the motors are not placed serially as the common method. Most of the mass concentrates in the anterior body to reduce the body recoil.

With the aid of pectoral fins and a swimming bladder, the real fish can swim freely in 3D space. In this paper, the pitching motion is achieved by two separate pectoral fins driven by servo motors with one degree of freedom (1-DOF). Main feature parameters of the developed robotic prototype are listed in Table II.

III. Open-Loop Control Method and Experiments

A. Open-Loop Control Method

For thunniform swimmers, elongated-body theory is not applicable. Because the body and caudal fin are airfoil profile, violating the basic assumption of slenderness. Normally, we consider that the propulsion are generated by an oscillating foil following a pitching movement in the thunniform swimming. However, it is worth pointing out that the different effort are caused by different driving mode. The real tuna uses muscular contraction and relaxation to drive the tail, so no or little torque works on the rigid anterior body. By contrast, the robotic one drives the tail mainly depending on the motor torque, which inevitably causes the body to swing more violently. Although this swing can be reduced by carefully choosing motion parameters, it still influences the swimming speed a lot.

It is difficult to mimic the swimming of a real fish exactly, for the fish has dozens of vertebras, which can be viewed as equal number of active joints. A practical way is to divide the robotic fish into several segments, and then apply the trajectory approximation method to calculate every joint angle through fish body wave fitting. But this method needs off-line calculation and hardly achieves a smooth transition between different swimming patterns. Another method is to use Central Pattern Generator (CPG) to control the joint angles. This method generates rhythmic signals online, and has advantages of easy adjustment, simple construction and quick implementation.

In this paper, we use a Hopf oscillator-based CPGs model to create control signals of joint angles. Fig. 2 shows the output of CPGs.

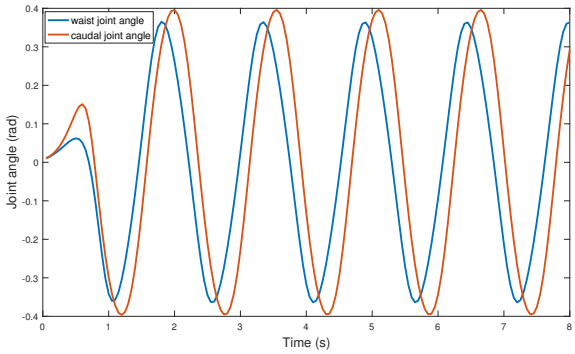

Fig. 2. Generated CPG signal.

$$\begin{cases} \dot{x_i} = -\omega\left(y_i - b_i\right) + x_i\left[A_i - x_i^2 - \left(y_i - b_i\right)^2\right] \\ \quad + h_1\left[x_{i-1}\cos\varphi_i + \left(y_{i-1} - b_{i-1}\right)\sin\varphi_i\right] \\ \dot{y_i} = \omega x_i + \left(y_i - b_i\right)\left[A_i - x_i^2 - \left(y_i - b_i\right)^2\right] \\ \quad + h_2\left[x_{i+1}\sin\varphi_i + \left(y_{i+1} - b_{i+1}\right)\cos\varphi_i\right] \\ x_i = y_i = b_i = 0,\ while\ i < 1\ or\ i > 2; \\ \theta_i = c_i y_i \end{cases} \tag{1}$$

where x_i and y_i are states of the ith oscillator; A_i and ω indicate the intrinsic amplitude and frequency, respectively; h_1 and h_2 denote the coupling weights, often expressed as constants; φ_i stands for phase relationship of neighboring oscillators; b_i is directional bias; c_i is used as amplification coefficient, and θ_i gives the expected angle of the ith joint.

By changing values of parameters in CPG model, it is easy to realize multiplex motion mode of robot.

B. Experiments of Straight Swimming and Turning

Experiments are conducted in an indoor pool. The dimensions of the pool are 5 m × 4 m × 1.3 m. A ceiling-settled global vision system is used to get accurate experimental data. The results are shown in Figs. 3 and 4.

In the experiments, the whole swimming processes are recorded, and then the colored parts are marked frame by frame as shown in Fig. 3(a) and Fig. 4(a). With the calculated mapping relations between the pixels and actual locations, we obtain digital descriptions as shown in Fig. 3(b) and Fig. 4(b). The maximum straight swimming speed is about 0.76 m/s (1.65 BL/s), and the minimum turning radius is around 0.16 m (0.35 BL). We can also learn from the Fig. 3(a) that it is difficult to swimming straight under open-loop control. Many reasons lead to this result, such as transmission clearance, heaving water caused by the robot, fluctuating anterior body, and so on. Thus, a closed-loop course control is needed to ensure a stable heading direction.

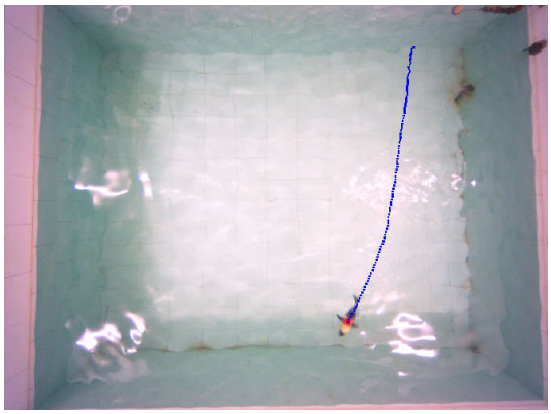

(a)

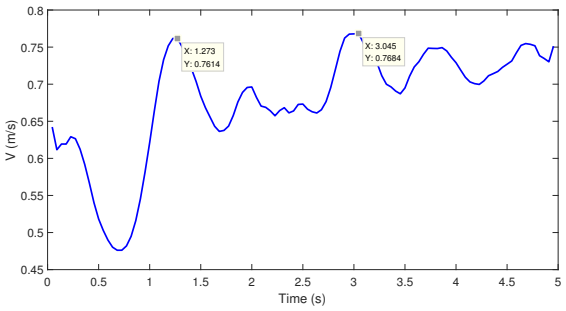

(b)

Fig. 3. Straight swimming test. (a) Snapshot of straight swimming. (b) Calculated speed of straight swimming.

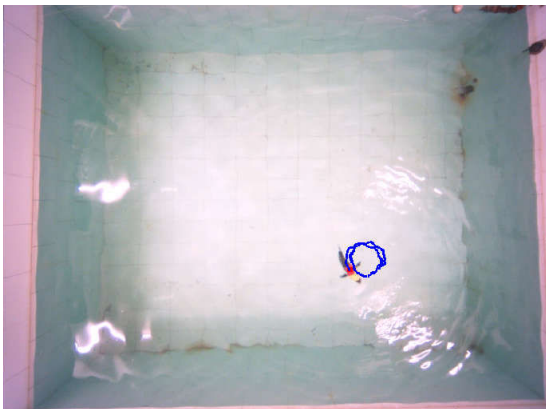

(a)

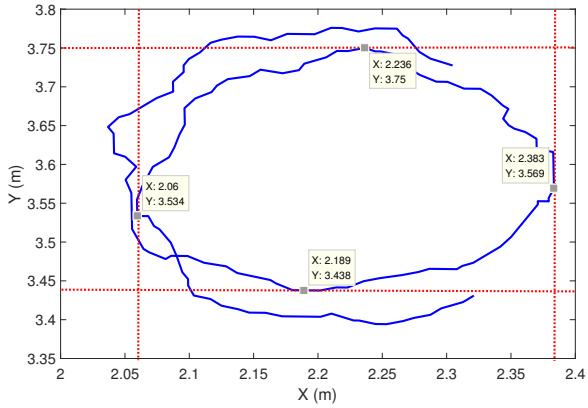

(b)

Fig. 4. Turning test. (a) Snapshot of turning. (b) Calculated data of turning.

IV. Yaw Control and Simulation

A. Yaw Control Method

Subtle asymmetric force will cause a deviation, when the robotic fish propels itself by interacting with surrounding water. In fact, due to the increasing forward swimming speed in the initial stage, symmetrical beats produce asymmetric force. The simulation result shown in Fig. 5 confirms this. Due to the swing of anterior body, instantaneous yaw angle does not indicate the real yaw angle. And complex hydrodynamics make it impossible to give an accurate description of the swing. But considering that the swing of anterior body is caused by both the surrounding water and rhythmical undulation of tail fin, we can infer that the swing will be symmetric when the robotic fish swims steadily. So, we can use the upper and lower bound of the measured yaw angle to approximate the actual yaw angle.

As illustrated in Fig. 6(a), θ_{ref} is the reference yaw angle, and θ_A defines the upper and lower bound. θ_{ins} denotes the instantaneous yaw angle of the anterior body. Then the yaw control method can be described by Fig. 6(b). If the measured θ_{ins} follows out of the range of $[\theta_{ref} - \theta_A, \theta_{ref} + \theta_A]$, for instance, reaches the upper bound (i.e.,$\theta_{ref} + \theta_A$), the robotic fish will turn right. Likewise, if θ_{ins} fluctuates over the lower bound (i.e.,$\theta_{ref} - \theta_A$), the robot will turn left.

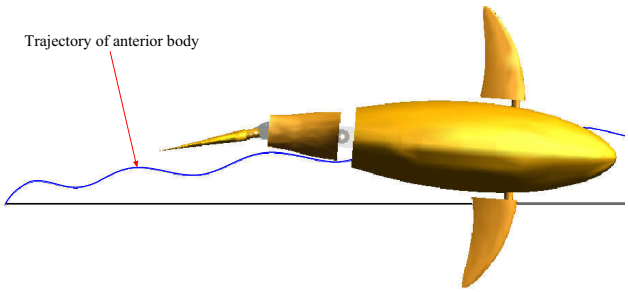

Fig. 5. Anterior body trajectory under open-loop control.

Considering the CPG mode given in previous section, b_i is used as directional bias in open-loop control. Here, a simple proportional-integral-differential (PID) algorithm is employed to regulate the value of parameter b_i to realize a closed-loop control of yaw angle. In this paper, we mainly consider the condition of $i = 1$, meaning that directional bias is used to control waist motor.

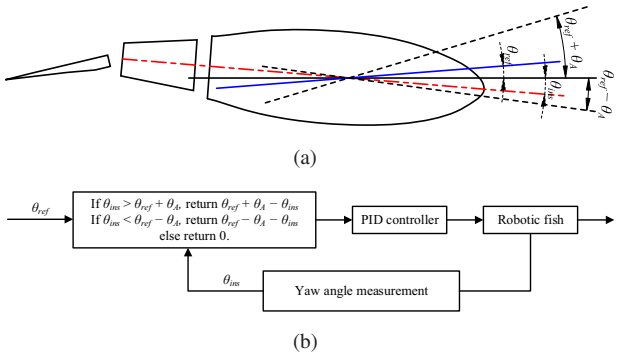

Fig. 6. Illustrations of the yaw control method.

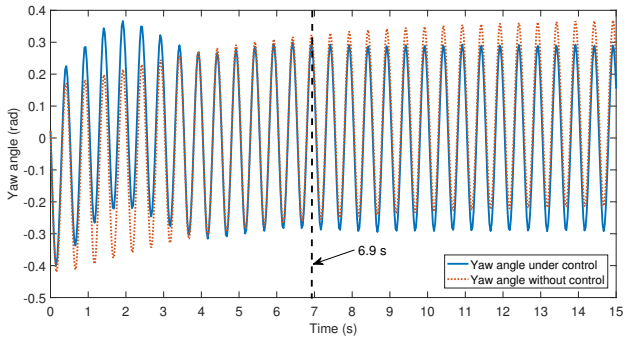

Fig. 7. Compared simulation results of yaw angles.

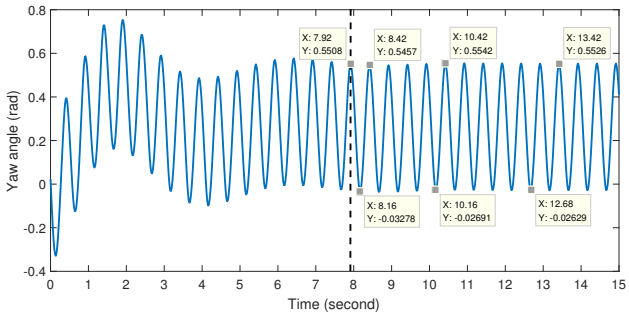

Fig. 8. Simulation results with $\theta_{ref} = \pi/12$ and $\theta_A = \pi/12$.

B. Simulation Analysis

The simulation is conducted by Automatic Dynamic Analysis of Mechanical Systems (ADAMS) software, mainly focusing on two aspects. One is to verify the effectiveness of proposed method, and the other is to find out the effect of θ_A.

At first, we set $\theta_{ref} = 0$ and $\theta_A = \pi/12$, the simulation results are shown in Fig. 7. It is easy to see that the robotic fish can not keep a steady swimming direction without yaw control. Though the body fluctuation makes it hard to recognize the real yaw angle, we can use symmetry of angle fluctuations to confirm it. Learning from the simulation result, the yaw angle fluctuation has trended steady and symmetrically after 6.9 s, indicating that the robot reaches the desired yaw angle.

Further, a simulation with $\theta_{ref} = \pi/12$ and $\theta_A = \pi/12$ is performed, and the returned result is illustrated in Fig. 8. Still, the actual yaw angle can not be recognized directly, but a simple method helps to calculate it. Observed from the Fig. 8, θ_{ins} fluctuates symmetrically after 7.92 s. The peak points and the lowest points after this time can be used to estimate the real yaw angle. The calculated result is 0.26, roughly equal to the given θ_{ref}, which not only verifies the validity of presented yaw control method but also confirms the judgment that steady and symmetrical fluctuation can be used to determine the value of actual yaw angle.

Next, simulations concentrate on the effect of different θ_A. While $\theta_{ref} = \pi/12$, the value of θ_A is set as $\pi/36$, $\pi/18$, $\pi/12$, and $\pi/9$ respectively. The result is shown in Fig. 9.

Some conclusions can be derived from the above simulations:

- Larger value of θ_A means a longer time to stabilize the fluctuation. It is reasonable, for the yaw control method only works when the value of θ_{ins} is out of the range. This means less influence on the swimming speed. Additionally, there is tiny difference of final speed between $\theta_A = \pi/12$ and $\theta_A = \pi/9$.
- Conversely, smaller value of θ_A makes the fluctuation reach the desired state quickly, with sacrificing in speed, as shown in Fig. 9(b). Considering an extreme condition of $\theta_A = 0$, θ_{ins} is used to control the turning directly, then the parameter b_1 will change all the time except for a few points. This condition may ruin the rhythmicity of tail motion, affecting the speed greatly.
- Although the proposed yaw control method can make the yaw angle fluctuate in a given range, sideways drift is unavoidable, as shown in Fig. 9(c). It is hard to eliminate the impact caused by the lateral force generated in the initial phase. A small value of θ_A helps the robot to converge quickly to a stable fluctuating state, but the existing lateral deviation can not be compensated.
- The course correction is achieved by adjusting the parameter b_1, impacting the waist motor directly, so the response of the yaw control is quick. However, the waist joint is restricted by the physical structure, so a large value of θ_{ref} may lead to motor locked. A number of gradually small adjustments may be a good method to deal with the sudden large input.

V. Conclusions and Future Work

In this paper, we have presented the design and control a novel two-motor-actuated robotic fish capable of both fast swimming and high turning maneuvers. More specifically, the robotic fish has a well-streamlined profile mimicking a tuna.

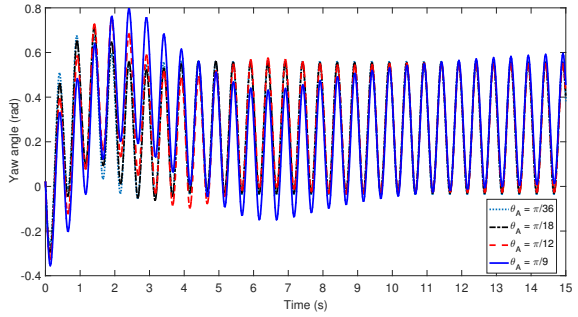

(a)

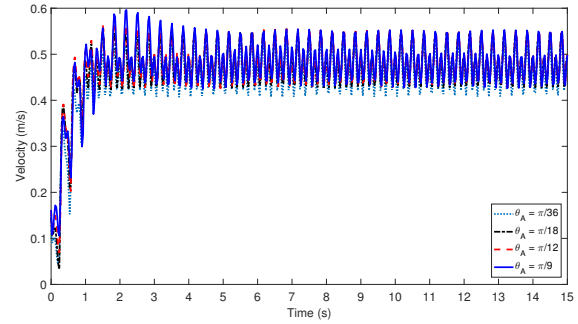

(b)

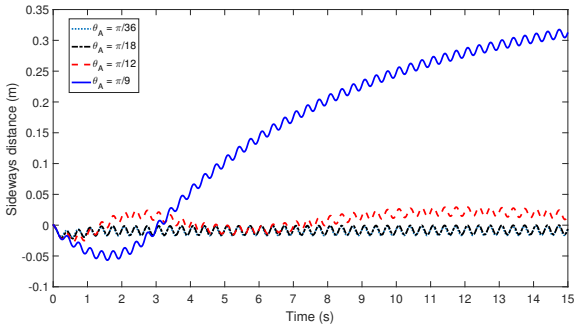

(c)

Fig. 9. (a) Yaw angles with $\theta_{ref} = \pi/12$ while θ_A is equal to $\pi/36$, $\pi/18$, $\pi/12$, and $\pi/9$ respectively. (b) Velocities with $\theta_{ref} = \pi/12$ while θ_A is equal to $\pi/36$, $\pi/18$, $\pi/12$, and $\pi/9$ respectively. (c) Lateral distances with $\theta_{ref} = 0$ while θ_A is equal to $\pi/36$, $\pi/18$, $\pi/12$, and $\pi/9$, respectively.

The narrow caudal peduncle brings great difficulties to the mechanical design. To overcome this problem, a two-stage transmission mechanism is adopted to drive the caudal fin. By placing both of the motors in the anterior body, volume and mass of active parts reduce a lot. 3D maneuverability is achieved by a pair of pectoral fins with 1-DOF. During experiments, the robotic fish peaked 1.65 BL/s and turned around within 0.35 BL under the open-loop control based on CPG. Furthermore, a yaw control method is proposed to deal with the problem of unstable swimming direction. The simulation results confirm the effectiveness of the proposed control method. Additionally, such results also reveal the fact that the proposed method can only correct the swimming direction, but incapable of dealing with the lateral deviation caused by asymmetrical lateral forces.

Our future work will concentrate on improving and applying this yaw control method for better turning ability. Meanwhile, we will combine the yaw control and embedded vision to achieve path following in real underwater environments.

REFERENCES

[1] M. Sfakiotakis, D. M. Lane, and J. B. C. Davies, "Review of fish swimming modes for aquatic locomotion," IEEE J. Ocean. Eng., vol. 24, no. 2, pp. 237–252, May. 1999.

[2] J. E. Colgate and K. M. Lynch, "Mechanics and control of swimming: A review," IEEE J. Ocean. Eng., vol. 29, no. 3, pp. 660–673, 2004.

[3] M. H. Dickinson, C. T. Farley, R. J. Full, M. A. R. Koehl, R. Kram, and S. Lehman, "How animals move: An integrative view," Science, vol. 288, no. 5463, pp. 100–106, 2000.

[4] Y. Zhong and R. Du, "Design and implementation of a novel robot fish with active and compliant propulsion mechanism," in Proc. Robotics: Science and Systems XII, Univ. Michigan, Ann Arbor, MI, USA, 2016, pp. 1–9.

[5] R. J. Clapham and H. Hu, "iSplash-I: High performance swimming motion of a carangifom robotic fish with full-body coordination," in Proc. IEEE Int. Conf. Robot. Autom., Hong Kong, China, May 2014, pp. 322–327.

[6] R. J. Clapham and H. Hu. "iSplash-II: Realizing fast carangiform swimming to outperform a real fish." in Proc. IEEE/RSJ Int. Conf. Intell. Robot. Syst., Chicago, IL, USA, Sep. 2014, pp. 1080–1086.

[7] S. Verma, J. X. Xu, Q. Ren, W. B. Tay, and F. Lin, "A comparison of robotic fish speed control based on analytical and empirical models," in Proc. 42nd Annu. Conf. IEEE Ind. Electron. Soc., Florence, Italy, Oct. 2016, pp. 6055–6060.

[8] Z. Wu, J. Yu, Z. Su, M. Tan, and Z. Li, "Towards an esox lucius inspired multimodal robotic fish," Sci. China Inform. Sci., vol. 58, no. 5, pp. 1–13, 2015.

[9] M. S. Triantafyllou and G. S. Triantafyllou, "An efficient swimming machine," Sci. Amer., vol. 272, no. 3, pp. 64–70, Mar. 1995.

[10] Z. Wu, J. Yu, and M. Tan, "CPG parameter search for a biomimetic robotic fish based on particle swarm optimization," in Proc. IEEE Int. Conf. Robot. Biomim., Guangzhou, China, Dec. 2012, pp. 563–568.

[11] S. Zhang, Y. Qian, P. Liao, F. Qin, and J. Yang, "Design and control of an agile robotic fish with integrative biomimetic mechanisms," IEEE/ASME Trans. Mechatronics, vol. 21, no. 4, pp. 1846–1857, 2016.

[12] A. Crespi, D. Lachat, A. Pasquier, and A. J. Ijspeert, "Controlling swimming and crawling in a fish robot using a central pattern generator," Auton. Robot., vol. 25, pp. 3–13, 2008.

[13] Y. Hu, J. Liang, and T. Wang, "Mechatronic design and locomotion control of a robotic thunniform swimmer for fast cruising," Bioinspir. Biomim., vol. 10, no. 2, p. 026006, 2015.

[14] J. Liang, T. Wang, and L. Wen, "Development of a two–joint robotic fish for real–world exploration," J. Field Robot., vol. 28, no. 1, pp. 70–79, 2011.

[15] J. Liu and H. Hu, "Biological inspiration: From carangiform fish to multijoint robotic fish," J. Bionic Eng., vol. 7, no. 1, pp. 35–48, 2010.

[16] Z. Su, J. Yu, M. Tan, and J. Zhang, "Implementing flexible and fast turning maneuvers of a multijoint robotic fish," IEEE/ASME Trans. Mechatronics, vol. 19, no. 1, pp. 329–338, 2014.